Numerical Study of the Parabolic Dish Solar Collector Performance Evaluation Using Heat Exchanger Receiver

Bassim M. Majel[1], Zain Alabdeen H. Obaid[2*], Khudir Zidane[3]

[1] Department of Refrigeration and Air-Conditioning Engineering, Al-Rafidain University College, Baghdad 10001, Iraq
[2] Renewable Energy Research Centre, University of Anbar, Ramadi 31001, Iraq
[3] Al-Anbar Sewerage Directorate Chief of Engineering, Anbar, Ramadi 31001, Iraq

Corresponding Author Email: zaobaid@uoanbar.edu.iq

ABSTRACT

The solar water heater is one of the most important applications used to invest in renewable energy, specifically solar energy, where hot water can be used for air conditioning, household uses, or industrial purposes. In this work, a new system was established for the production of hot water and steam using solar concentrators of the solar dish type, made of aluminum, having a (175 cm) diameter and a deepness of (15 cm) with a heat exchanger (radiator) as a receiver which is a new and innovative way of working. The front side of the dish was covered with strips of nickel metal reflecting sunlight to focus the solar radiation on a tank fixed at the center of the focus of the rays reflected from the dish. A heat exchanger (radiator) was used as a tank with the following dimensions (50cm×40cm×5cm) and a capacity of (4 liters). Numerical calculations were carried out using (Solidworks) and (Ansys workbench) to design and analyze this system. The simulated data revealed that the focus's placement and the spacing of the dishes are governed by the dish's size and the degree of inclination. The concentration ratio increases by (53%) when the dish diameter increases. The use of a radiator heat exchanger gives the largest use of solar-reflected radiation that is reflected from the collector because of the increased surface area exposed to solar radiation due to the presence of fins. The highest thermal efficiency (72.16%) was obtained at 355 K and a mass flow rate of 0.32 kg/sec.

1. INTRODUCTION

Today, the globe is currently experiencing an economic crisis as a result of rising energy costs and growing demand for fossil or conventional energies (oil, gas and coal). Fossil fuel resources are in short supply. Furthermore, greenhouse gas emissions pollute the ecosystem, which resulted in heat attrition, height temperatures, acid rains, fusion snow, submerged agricultural earth, and other areas' depletion, all of which contributed to desertification. This increases reliance on renewable energy sources, with solar energy being the leading contender for remembrance of this type of energy because of its great availability, cheap cost, as well as the fact that it represents a "clean energy source". It is also quite simple to provide when carried from the world's well-known "solar belt." (Countries like Iraq) to the population centres of the earth [1]. The energy received from the sun in one year is twice as much as the user, discovered and estimated from the energy of coal, oil, gas and uranium nuclear energy. Solar energy may be used in two ways: solar thermal, which is the process of turning solar energy into heat energy using a solar thermal collector. The second way is solar electric power, which converts solar radiation directly into electrical energy through the use of solar panels or cells [2]. Concentrating solar energy system (CSES) is the process of harvesting and exploitation of solar energy to produce thermal energy and uses concentrates or solar thermal collectors (solar thermal collectors) for this

purpose [3].

Soteris [4] published research about thermal collectors that harvest solar energy. They also presented the utilization of the sun's energy and its applications. Moreover, kinds of collectors such as flat plates, Compound parabolas, evacuated tubes, heliostat field collectors, Fresnel lens, parabolic trough, and parabolic dishes are all examples of field collectors for heliostats the collectors' optical, thermal, and thermodynamic properties were then analyzed, as well as the methodology used to assess their performance. The consistent employment of several types of collectors was proven, taking into account the breadth of their uses.

According to Wu et al. [5], the general thermal-electric transition performance of a parabolic dish/AMTEC solar thermal power framework was evaluated. A consolidated framework was used to connect a parabolic dish solar collector to an Alkali Metal Thermal to Electric Converter (AMTEC) using a coupling heat exchanger. A different kind of heat pipe receiver was used to isothermally transfer the solar energy from the collector to the AMTEC. A hypothetical examination similar to a parametric examination was performed to evaluate the framework's general thermal–electric transformation performance by modifying significant characteristics, including performance variables related to the dish collector and the AMTEC as well as the average temperature. According to the results, a parabolic dish/AMTEC system with a productivity of 18.54 kW and a temperature of operation of

1280 K could achieve a conversion efficiency of up to 20.6%. Furthermore, it is discovered that the ideal condenser temperature, which corresponds to the highest overall efficiency, is somewhere between 600 K and 650K.

Dascomb [6] provided a comprehensive description of the economic collector that was utilized for producing steam. The study compared it with other methods of renewable giving 80% preferred execution over some other technology and generally cost is the least. The objective of the venture was to provide 6.67 kW of thermal energy. This is the measure of the energy required to create 1 kW of power with a regular, smaller-scale steam turbine. The framework had a value objective of $1000 per kW and must be sufficiently straightforward to keep up with non-specialized staff. To ensure simplicity of generation and operation, a 14 m^2 fiberglass parabolic concentrator was developed at SESEC. A very responsive polymer lm is used to cover the concentrator. The cavity is made up of a receiver that is filled with sodium nitrate to serve as a medium for storing and transferring heat. The efficacy of cavity collection was 70%. The system's gross thermal conversion efficiency, which was 39 percent, was 33 percent higher than that of the first concentrator put together at SESEC. The thermal energy of 5.46 kW was generated at the pinnacle insulation.

Madadi et al. [7] fulfilled the design, construction, and test requirements of a parabolic dish collector (PDC) to study the exergy and energy performance theoretically and experimentally. Investigations are conducted into the effects of solar radiation, the receiver aspect ratio, the receiver temperature, the receiver type, the heat transfer fluid's mass flow rate, and the inlet temperature. The fully opened receivers are inferred to have the highest energy and thermal efficiency. The receiver of cylindrical shape has greater exergy and energy efficiency than the conical one due to minimal exergy devastation. According to studies, between 35% and 60% of all exergy is lost, this is because of heat transport between the sun and the receivers, which also causes the most exergy destruction. Li and Dubowsky [8] developed a PDC, in which the mirror of the dish consisted of petals of thin flat metal that optimized the reflective capacity of the parabola. In this system, temperatures of 120°C were found in the stream of water.

Lovegrove et al. [9] a newly developed 500 m^2 parabolic concentrator of solar energy with a 13.4 m focal length and altitude-azimuth tracking. The design involves using thirty-eight spherical mirrors that are the same. These mirrors are 1.17 meters and use the glass metal laminate mirror. According to the findings of the study, employing these receivers with it should be feasible to achieve a high concentration ratio of more than 200 times. Moreover, the experimental test gives the results listed in Table 1.

Table 1. Summary of experimental run carried out on the 6th of August 2010 for lovegrove work [9]

Mass Flow [g/s]	Outlet Temp [°C]	Outlet Steam Power [kW]	Receiver Thermal Efficiency [%]
97	502	333	85
120	283	357	92
129	177	362	94

Mohammed [10] designed a PDC for domestic applications, in which 40 liters of water at more than 100°C were daily provided to a family with 25% - 56% of thermal efficiency.

Following the sun using a linear actuator (Super jack) reduces the necessity for regular monitoring by an operator, lowering labour costs. The cylinder receiver type was utilized. It was discovered that the coefficient of convective heat losses improved by roughly 25 to 41% as the absorber temperature rose from 150 to 200°C.

Rafeeu and Ab Kadir [11] constructed three test models with varying geometrical shapes, and solar dish concentrators with 0.5 m diameters were employed to investigate geometry's influence on solar irradiance and temperature, as well as to maximize the solar intensity in Malaysian circumstances. These models were employed in order to investigate the parabolic concentrating collector's characteristics, such as reflector materials, aperture diameter, concentrator depth, focal point size, and focal point temperature, with varying solar irradiation to raise thermal efficiency. The efficiencies were computed, and the findings were unmistakable. Silverlux aluminum sheets with a thickness of 3mm were significantly more productive than hardened steel and increasing the concentrator zone resulted in far more significant variances in the results. The spiral copper coil was used as an absorber. The efficiencies are calculated, and the results are conclusive. When compared to stainless steel, the 3 mm Silverlux aluminum films are more effective and expanding the concentrator's surface area causes results-specifically, efficiency-to to vary significantly more from base to top. Overall, D1 and D2 are more efficient than D3, which, when losses are taken into account, is frequently only 50%.

Karimi et al. [12], the functioning principles of two contemporary compound parabolic trough and dish solar collectors were introduced. The mirror curves were clarified, and the use of mathematical formulation as one analytical technique to track the sun's rays and identify the focal point. The distribution of heat flux around the inner wall will be achieved as a result of ray tracing. Heat flows were calculated about various absorption coefficients. In a polar coordinate system, these changes in heat flow around the absorber tube are functions of an angle. As a thermal boundary condition, the obtained heat flux fluctuations are applied. The simulation of the absorber tube was done using finite volume techniques. Some of the attributes of the LS-2 and two current-built collectors are regarded as an equivalent for a fair comparison. For modelling the modern provided collectors, factors such as the aperture area, the operating liquid, the thermal characteristics of the absorbent tube, the measurements of tube geometry, the mass flow rate of the LS-2 collector and the solar radiation intensity were used. The comparison findings revealed that the efficiency of the newly constructed parabolic collectors had improved. The efficiency benefits in the best case study were around 10% and 20% for linear and convoluted models, respectively.

A solar parabolic dish created by Sakhare and Kapatkar [13] is being employed in applications for cooking and water heating. This study had its basis in the development of a steam generation system using a non-tracking solar paraboloidal dish, which was highly reflective due to the utilization of aluminum as a fabrication material. The development of a steam generation system for rural areas was encouraged by these findings. Copper tube was used to absorb solar energy whose position suppressed the need of tracking the sun in the east-west direction while optimizing the tracking in the north-south direction. All these experiments were executed on cloud-free days, resulting in a measure of 215°C as the temperature of the steam stream and an efficiency of 60%.

Sada and Sa'ad-Aldeen [14] dealt with the concentrated solar dishes that are used to generate steam from solar energy. Solar radiation strikes the dish and is reflected in an absorbing vessel containing the water-carrying helical coil. The findings of this experimental effort indicate that it is possible to generate steam from sunlight in Iraq for a short period. This assessment was completed in September of the year 2014 by noon, when the solar irradiation was about to reach its maximum, increasing the temperature of a stream of water from 38°C to 115.7°C in several minutes. The experimental data show that could be produced superheated steam when increasing the length of the receiver coil.

Mahmood et al. [15] used a (52) plane mirror to design and construct a (3.25 m) solar dish array. To reflect the radiation in a single region (focus) at a distance, these mirrors were levelled and fastened (1.5 m). Additionally, it was discovered that the center's efficiency is 55 percent at (400-700 W/m^2) and that the heat concentration is (217.79 W), but the useable energy is (1416.125 W). It was shown that the efficiency of the center at (400–700W/m^2), useful energy (at 1416.125 W), and heat concentration (at 217.79 W) were all at 55%. For solar thermal applications, the solar dish array is largely appropriate. The solar dish array has proven to be an excellent choice for solar thermal applications.

Khan et al. [16] examined numerically a parabolic dish cavity receiver with three different nanofluids, and the dish system was coupled with an s-CO$_2$ Brayton cycle to generate electricity. According to the findings, Al$_2$O$_3$ oil-based nanofluid has the highest overall energy and exergy efficiencies, coming in at nearly 33.73% and 36.27%, respectively. It is also nearly 0.27% more efficient than TiO$_2$ oil-based nanofluid and nearly 0.91% more efficient than CuO oil-based nanofluid. Investigations are also conducted into how wind speed affects receiver effectiveness.

Parabolic dish solar collectors were used by Khan et al. [17] to examine the thermal conversion efficiency because of their maximum concentration ratio. The working fluids in the parabolic dish solar collector that have been studied include supercritical carbon dioxide, therminol VP1, and pressurized water. By adjusting the working fluid's inlet temperature and flow rate in the parabolic dish solar collector, the current study aims to determine the ideal operating conditions for each heat transfer fluid. It is predicted that the interaction of these parameters will result in the collector's maximum output and energy efficiency. To investigate the overall system efficiencies, work output, and process heating rate, the operating parameters are changed. According to the study's conclusions, therminol VP1 is effective for a wider temperature range than water at low-temperature levels for heat transfer. The integrated system efficiencies are higher at maximum flow rates and low inlet temperatures. The study's efficiency map for the solar collector can be found there; it shows that at an inlet temperature of 750K, the maximum energy efficiency gains are observed to be 37.75%.

Mari et al. [18] used MATLAB to model and simulate a standalone solar parabolic dish Stirling system to study how material design and opt- geometrical parameters affected the system's output performance. The main parameters taken into account for the investigation include the concentrator diameter, rim angle, dispersion angle, incidence angle, solar angle, receiver emissivity, receiver absorbance, receiver thermal conductivity, and concentrator reflectance. In order to determine the ideal geometrical arrangement of the system, the optimized values of the investigated parameter have also been

identified. According to the findings, the system's overall efficiency and maximum output power were calculated at 45° rim angle, 0.4° dispersion angle, 0° incidence angle, and 0.3° solar angle. The results were also compared with theoretical and experimental datasets from recent literature for validation purposes and found to be in good agreement.

It is presented there are many studies about the performance investigation of parabolic dish solar collectors but there is a lack of studies concerning the use of a car radiator as a receiver to increase the efficiency of the solar collector. The aim of the present research is to examine in detail the increasing outlet receiver temperature which will affect the thermal efficiency of the solar collector using pressurized water as heat transfer fluids. The thermal energy produced by the collector is further utilized to power a regenerative steam cycle for the purpose of electricity generation and rate of process heat or for domestic usage. Various inlet temperature levels and mass flow rates are investigated to evaluate the process heat rate and the collector performance. Different combinations of temperature and flow rate are tested for each heat transfer fluid, and at the end, a unique method of solar efficiency map is presented to depict the efficiencies of the solar receiver. This work presents a numerical study of concentrating solar systems (PDC) in Iraq. The location of Iraq in a hot arid region and the high intensity of solar radiation helps. The shortage of electricity in Iraq leads to utilizing solar energy to heat water because solar energy is clean, cheap and available. The purpose of this action is to look into numerically the effectiveness of (PDC) by using a special type of receiver tank and different flow rates by studying: the effect of parabolic dish diameter on the focus point position, the effect of reflective material types on concentration ratio and the effect of receiver tank shape on the outlet temperature and pressure of water or steam.

2. SOLTRACE OPTICAL STUDY

A Monte-Carlo ray-tracing software program called SolTrace is available for download from the website (NREL) [19]. Both Windows and Mac OS X operating systems support it. The Spencer and Murty theory are the one put forth [20]. Icons to open windows for various stages in the creation and execution of a ray-tracing simulation can be seen on the far left. A three-dimensional ray-tracing simulation can be seen on the right. The view into the page is to the north, the positive x-direction is due east, and the positive y-direction is vertical. Individual rays (yellow lines) are depicted as they travel from the sun (at a roughly 45° angle) downward, reflecting off the mini heliostat panels (bottom right of the white grid), moving up to the beam-down mirror (top left of the grid), and then vertically downward into the calorimeter.

The steps involved in the definition of the SolTrace model and its run execution include the definition of the sun's shape, its optical properties, and the system stages that define the ray-tracing model. The different optical characteristics must be entered in a dialogue box. In this case, the reflecting material (nickel sheet metal) is calculated to have a reflectivity of 0.82 and a transmissivity of 0.2. Another new addition to SolTrace is the capability to specify the geometry using Trimble Sketch Up, a free three-dimensional (3D) modelling program (formerly Google Sketch Up). A Sketch-Up SolTrace plug-in enables the generation of elements and stages by SolTrace and is imported directly into SolTrace. The system may be tracked after it is specified. The user can choose how many rays should

be tracked via the system. This number is determined by how much information is required for findings. For instance, Optical efficiency data may be generated using fewer rays than a full flux map. Generally, flux mapping requires ray counts in millions. The system tracing findings can be viewed in various ways. View three-dimensional scatter plots of ray crossings with various components, with or without the displayed ray path. Flux maps can also be constructed on planar or cylindrical components. Centroids, peak flux, peak flux uncertainty, average flux, and other statistical data are visually generated and displayed. SolTrace data, including ray intersection positions and directions at different components, can be saved to a file for further use in reporting and/or post-processing using other tools.

3. COMPUTATIONAL ANALYSIS USING ANSYS PACKAGE

Computational Fluid Dynamics (CFD) is the use of computer-based simulation for the analysis of systems involving fluid flow, heat transport, and related phenomena. A mathematical model is first constructed using a collection of mathematical equations describing the flow. These equations are then solved numerically by a computer program to yield the flow variables over the flow domain. CFD development and use have grown significantly, and as a result, it has become a strong tool in engineering and other processes of design and analysis [21]. A solution of the continuity, Navier-Stokes, and energy equations are needed to analyze the flow field in a finned tube heat exchanger under conditions of constant heat flux, inner forced convection, conduction through the tube material, and outer free convection The governing equations for the actual setup cannot have an analytical solution due to the complexity of the geometry taken into account. Numerical simulations of the intricate geometry of the flow domain and the interaction can be used to conduct analyses. Therefore, finite volume numerical techniques by ANSYS-Workbench Fluent Code 17.0 [22] have been used to solve those equations. A single-phase is considered inside the heat exchanger.

3.1 Fluid flow governing equations

3.1.1 Continuity equation
The fluid conditions inside the storage tanks are predicted using computational fluid dynamics (CFD) in this study. During the numerical procedure, the governing equations are solved and the results are evaluated.

The mass- and momentum-conservation equations must be solved for flows modelled using CFD. The continuity or mass equation for a 3D geometry is obtained from Eq. (9) [21]:

$$\frac{\partial \rho}{\partial t} + \frac{\partial}{\partial x}(\rho u_x) + \frac{\partial}{\partial r}(\rho u_r) + \frac{\rho u_r}{r} = S_m \tag{1}$$

where, r is radial coordinate, x is axial coordinate, u_r is radial velocity and u_x is axial velocity. S_m is a source word that refers to the mass subjoin to the continuous phase from the dispersed second phase (like the vaporization of the liquid droplet) and any other user-defined source.

3.1.2 Navier-stokes equation
The equation of Navier-Stokes connects the viscous stress and deformation components in the equation of momentum

conservation. Eqns. (2) and (3) define the Navier-Stokes equation for a three-dimensional geometry [21]:

$$\frac{\partial}{\partial t}(\rho u_x) + \frac{1}{r}\frac{\partial}{\partial x}(r\rho u_x u_x) + \frac{1}{r}\frac{\partial}{\partial r}(r\rho u_r u_x) =$$
$$-\frac{\partial p}{\partial x} + \frac{1}{r}\frac{\partial}{\partial x}\left[r\mu\left(2\frac{\partial u_x}{\partial x} - \frac{2}{3}(\nabla \cdot \vec{u})\right)\right] + \frac{1}{r}\frac{\partial}{\partial r}\left[r\mu\left(\frac{\partial u_x}{\partial r} + \frac{\partial u_r}{\partial x}\right)\right] + F_x \tag{2}$$

$$\frac{\partial}{\partial t}(\rho u_r) + \frac{1}{r}\frac{\partial}{\partial x}(r\rho u_x u_r) + \frac{1}{r}\frac{\partial}{\partial r}(r\rho u_r u_r) =$$
$$-\frac{\partial p}{\partial r} + \frac{1}{r}\frac{\partial}{\partial x}\left[r\mu\left(\frac{\partial u_r}{\partial x} + \frac{\partial u_x}{\partial r}\right)\right] + \frac{1}{r}\frac{\partial}{\partial r}\left[r\mu\left(2\frac{\partial u_r}{\partial r} - \frac{2}{3}(\nabla \cdot \vec{u})\right)\right] \tag{3}$$
$$-2\mu\frac{u_r}{r^2} + \frac{2}{3}\frac{\mu}{r}(\nabla \cdot \vec{u}) + \rho\frac{u_z^2}{r} + F_r$$

where, u_z is the swirl velocity, μ is the dynamic viscosity, F_x and F_r are source terms and $\nabla \cdot \vec{u}$ is obtained by:

$$\nabla \cdot \vec{u} = \frac{\partial u_x}{\partial x} + \frac{\partial u_r}{\partial r} + \frac{u_r}{r} \tag{4}$$

3.1.3 Energy equation
The energy equation must be solved to solve problems with heat transfer. The equation can be obtained in Eq. (5):

$$\frac{\partial}{\partial t}(\rho E) + \nabla(\vec{u}(\rho E + p)) = \nabla\left(k_{eff}\nabla T - \sum_j h_j \vec{J}_j + \left(\bar{\tau}_{eff} \cdot \vec{u}\right)\right) + S_h \tag{5}$$

where, $\bar{\tau}_{eff}$ is the effective stress tensor, k_{eff} is the effective conductivity, $\vec{J}_j$ is the diffusion flux of species j and:

$$E = h - \frac{p}{\rho} + \frac{u^2}{2} \tag{6}$$

where, sensible specific enthalpy h is characterized for ideal gases as:

$$h = \sum_j Y_j h_j \tag{7}$$

3.2 Assumptions of finned tube heat exchanger

In this model, the following presumptions are made:
(1) Stable three-dimensional laminar and turbulent flow with single-phase fluid on the working side (homogenous model).
(2) An incompressible fluid that is Newtonian.
(3) Maintaining the same inlet temperature while ignoring viscous dissipation.
(4) The changes in kinetic and potential energy are insignificant.
(5) The axial conduction along the tube is usually insignificant.
(6) No heat generation within the heat exchanger, and the energy dissipation is within allowable limits.

3.3 Geometry system and solving processors

A SolidWorks Premium 2015 is used to draw the geometries of this work, which consist of a finned tube with inlet and outlet portions and a fluid tank on each side as shown in Figure 1. The outside flow is confined by a big environment with free convection. The flow is solved using three processors, which conserve energy in a finned tube heat exchanger as follows: The geometry is drawn by using SolidWorks

Premium software. It is exported as a Parasolid extension type to the ANSYS Workbench software program to create mesh and boundary conditions. Then, the geometry with mesh was added to the Fluent Package to solve and analyze the flow specifications. For simulating the focused sun-rays, there is a fourth processor named SolTrace software.
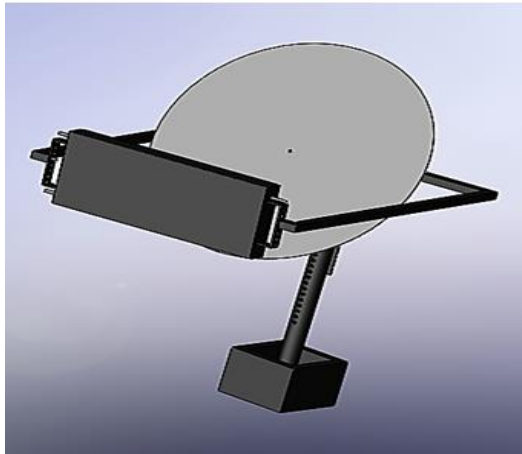

Figure 1. Photo of numerical test rig

3.4 Geometry creation with meshing

A heat exchanger is used as the geometry. ANSYS Workbench is used to create the 3-D geometry for the solid and fluid parts. The geometry is meshed using the unstructured meshing method, as seen in Figure 2.
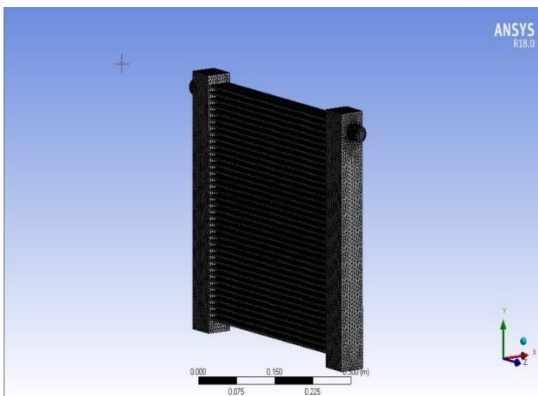
Figure 2. Meshing of receiver geometry

Grid generation is the process of dividing the domain into small elements. There are several different types of grids, including hexahedral, tetrahedral, prism, etc., based on the shape of the elements. A mesh that fits the bounds of the computational region is necessary for standard CFD algorithms. Research has long been focused on creating computational meshes that are appropriate for the discretized solution of three-dimensional conservation, continuity, momentum, and energy equations. The puzzles' geometries are carefully designed. The software packages SolidWorks and ANSYS workbench are used to model and mesh the case, respectively. Additionally, Fluent has a CFD application that gives the user total flexibility to adapt to suitable complicated geometry. To forecast the heat transport in intricate geometries, the grid system's development and refining are crucial. In other words, accuracy is greatly influenced by the density and dispersion of the grid lines [23-29]. ANSYS-Fluent 17.0, a commercial CFD software tool, is used to run numerical simulations. Checking the mesh/grid for faults is the first thing done when importing the mesh geometry into Fluent. Verifying the grid ensures that all zones are present and that all measurements are accurate. After the grid is established, the system's solver and boundary conditions are configured, and the case is then run and examined.

3.4.1 Grid independence solution

Four various grid densities were tested for the three-dimensional model, to ensure a grid independence solution. The corresponding numbers of elements were (312,668, 400,00, 410,534, and 470,652), elements, respectively. The compared consequence shows that the (410,534 elements and 97,867 nodes) are appropriate because it represents the superior compromise between the computational cost and the solution accuracy as shown in Figure 3. After reaching a successful mesh, the models were exported to Fluent for setup and analysis processes.
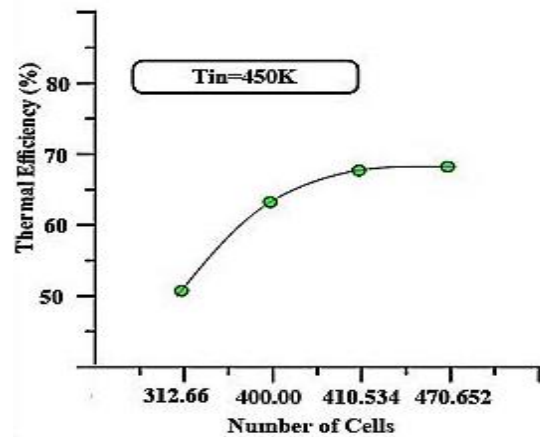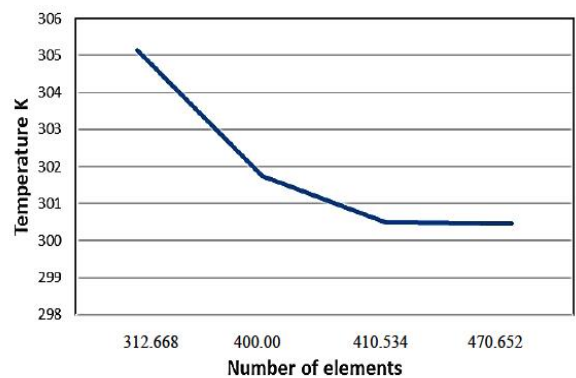

Figure 3. The grid independent solution test

4. RESULTS AND DISCUSSION

A commercial CFD program (ANSYS 18/Fluent) carried out numerical results using the finite volume method single-phase model for the case of a continuous flow rate with a uniform heat flux range (1000 W/m^2) for the front side (focused), ambient temperature (40℃), inlet water temperature (30℃) and heat transfer coefficient (30 W/m^2.K) with flow rate (32 L/hour).

4.1 Test section temperature distribution

The temperature distribution along the test section is shown

in three dimensions in Figure 4-a. The temperature profile at the inlet and outlet can be seen in Figure 4-b. By using approximately the same boundary condition as the experimental test, the theoretical result showed a good agreement. The results obtained revealed that the system could be used with a constant flow, and they were close to the experimental results, where the temperature of the outside water reached (80°C).
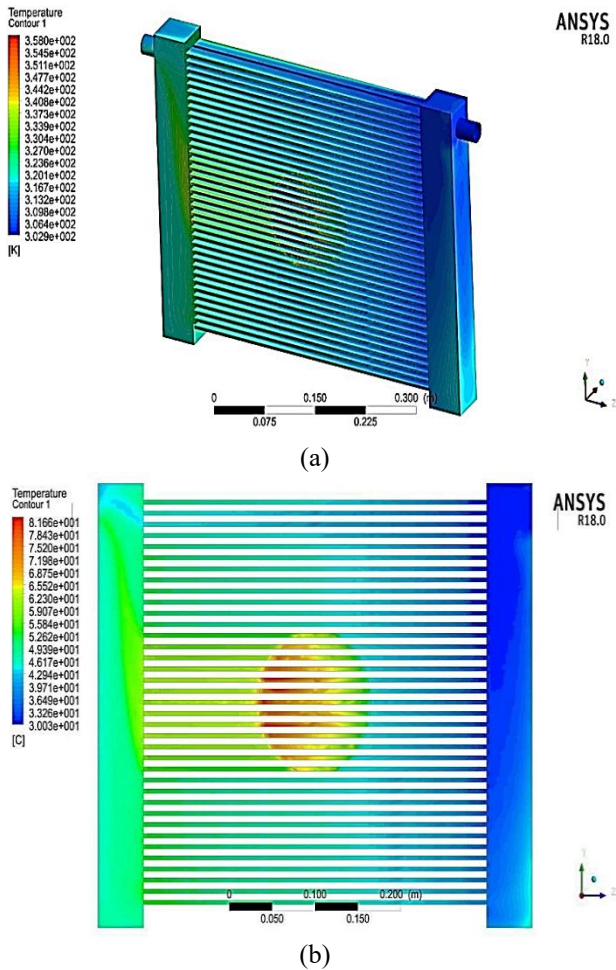

(a)

(b)

Figure 4. (a) 3-D temperature distribution along the test section; (b) Inlet and outlet temperature contour

4.2 Temperature of receiver (Radiator)

Table 2. Numerical results for the (PDC)

Dish	Heat exchanger receiver
Plant location	Iraq / Baghdad
Outlet fluid state	Steam
Dimensions of the receiver	(50 ×40 ×5) cm
Receiver tank capacity	4 litre
Water inlet temperature	33°C
Water outlet temperature	113°C

The numerical measurements from the receiver are shown in Table 2. In this type of receiver, simulations were carried out many times and during different weather conditions during the year. The results obtained for pressure and temperature are shown in Figures 4–11. These figures indicate that there are similarities in the results with a constant increase in the outside pressure and temperature of steam as one goes toward summer to reach the greatest value during July where the temperature

and pressure of the outside steam on 24/7/2021 at 3:49 were up to (121°C) and (1.3 bar) sequentially.

Figures 5 and 6 show how to ensure the temperature of the input stays unchanged throughout the simulation time when the water temperature within the receiver progressively rises over time until it reaches its peak at (11:12 am), (2:20 pm) about (105°C) and (116°C), respectively. Figure 7 demonstrates the pressure within the receiver, where all simulations were performed, does not rise higher than (1.4 bar) to prevent the receiver from being damaged, and the increasing pressure produces leaks through the receiver's welding regions. The maximum simulated values of pressure are (1 and 1.2 bars) at (11:12 a.m., and 2:17 p.m.) respectively. Figure 8 for May is predicted to behave similarly to April, despite differing values. The temperature was recorded after 20 minutes will reach (117°C). It climbed to the same level in April (113°C). Figure 9 shows the minimum and maximum outlet pressure at different periods, where the maximum recorded value is (1.25 bar) at (3:25 p.m.).

During the simulation that was conducted in July, it was found that there is a difference in the temperature at the beginning of the simulation between Figures 10 and 11 because the whole system reaches a high temperature at a steady state on sunny days. While, the pressure behaves the same and reaches its minimum zero value, Figure 12. This time decreases continuously during the simulation because of the intensity of reflected radiation on the receiver surface and the influence of the solar ray flux on the reservoir material, and thus heating the whole system.
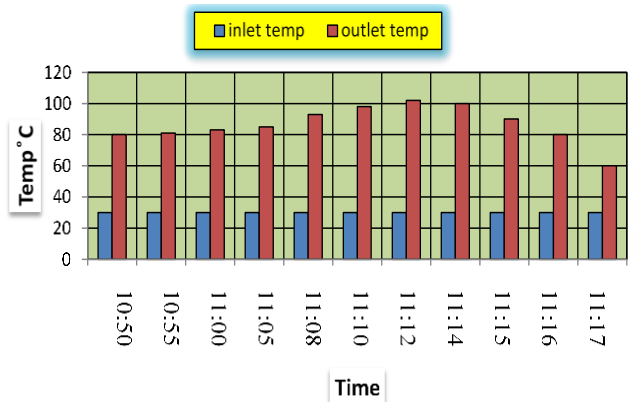

Figure 5. Numerical data of inlet and outlet temperature, test (1) (17/4/2021)
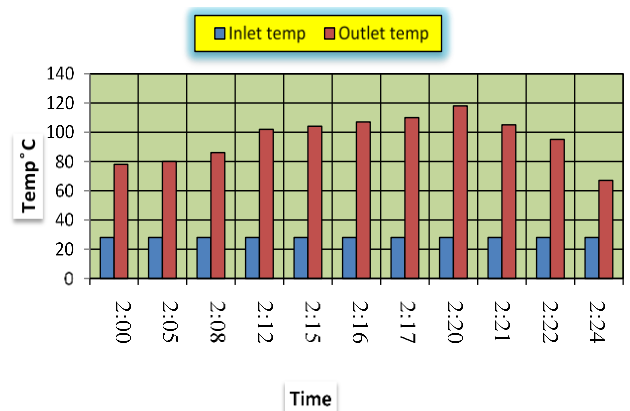

Figure 6. Numerical data of inlet and outlet temperature, test (2) (17/4/2021)
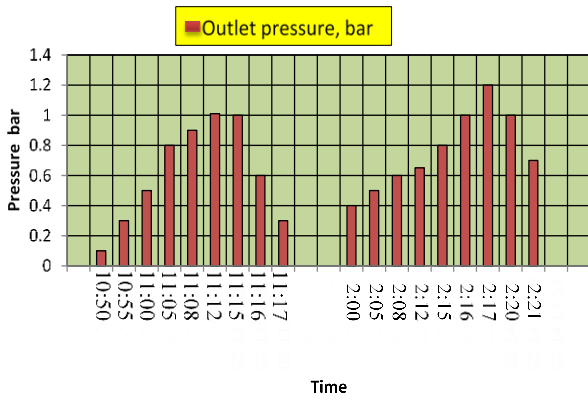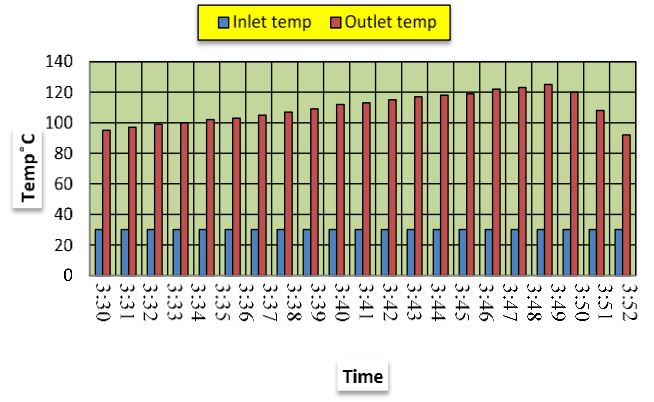
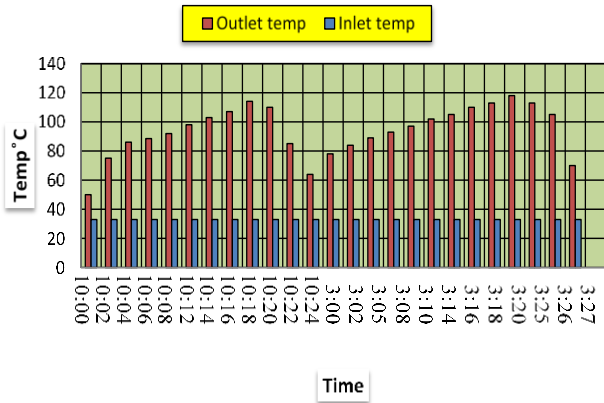**Figure 7.** Numerical data of outlet pressure, (17/4/2021)

Figure 8. Numerical data of inlet and outlet temperature, (25/5/2021)

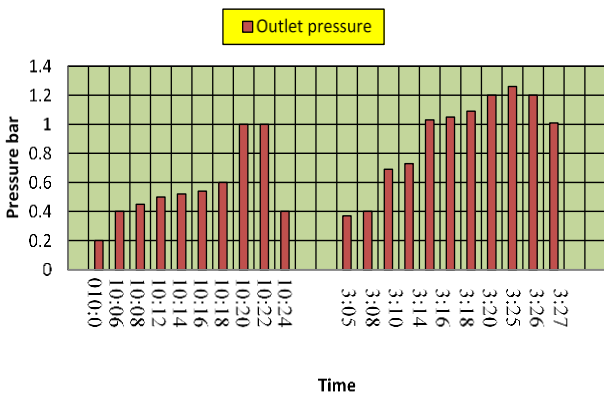**Figure 9.** Numerical result of outlet pressure, (25/5/2021)

Figure 10. Numerical result of inlet and outlet temperature, test 1 (24/7/2021)
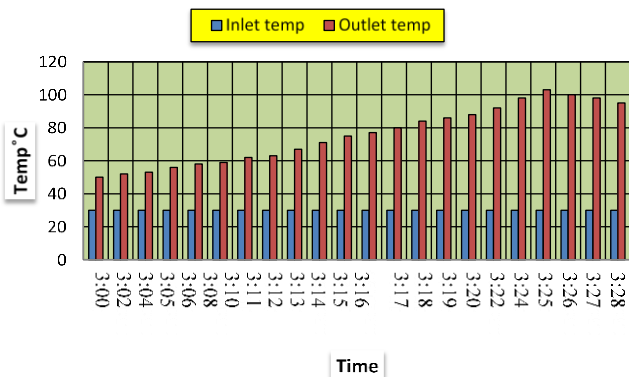

Figure 11. Numerical result of inlet and outlet temperature, test 2 (24/7/2021)

4.3 Hot water with continuous flow rate

A Possible use of this system is to obtain hot water with a continuous flow rate. When the simulation was conducted in August, two tested cases were relied upon: The first tested case was when the flow rate is (30 L/hour); it obtained hot water at a temperature between (59-64℃). In the second case when the flow rate is (40 L/hour); it obtained hot water at a temperature between (49-58℃). Therefore, it is possible to use this model as a solar heater or collector.

4.4 Comparing the Simulation results with practical experiments

The comparison between the simulated data with previous work in the literature is shown in Figure 12, and Table 3. For the thermal efficiencies, there are good agreement between the simulated results and practical data, and the maximum deviation data not exceed 9%.
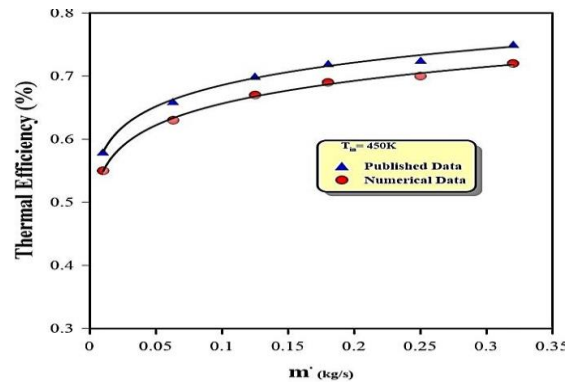

Figure 12. Comparison of experimental published data and numerical results

Table 3. Results of previous experiments related to the parabolic dish collector

Design Characteristics	Ihab [30]	Present Work
Location	Karbala/Iraq	Baghdad/Iraq
Radiator dimensions	(37×47×4) cm	(50×40×5) cm
Water inlet temperature	35℃	33℃
Water outlet temperature	65℃	75℃
Concentration ratio	76.8	80.6
Dish diameter	1.5 m	1.75 m
ΔT	36℃	42℃

4.5 Thermal efficiency of PDC

Through the study, it was found that the efficiency of the solar collector increases with the increase in the flow rate of the incoming fluid, as shown in Figure 13. It is also noted that the efficiency is directly proportional to the temperature of the incoming water. The higher the temperature, the higher the thermal efficiency. The highest efficiency was recorded at temperature of 450 K at a flow rate (0.32kg/s), as shown in Figure 14.
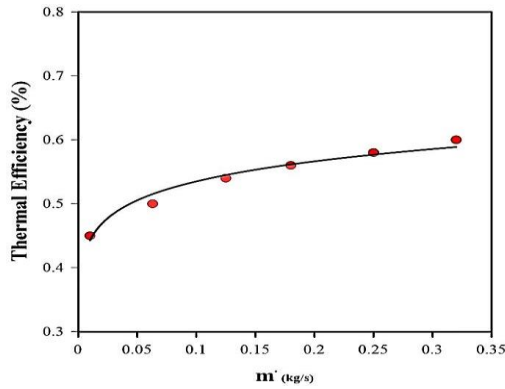

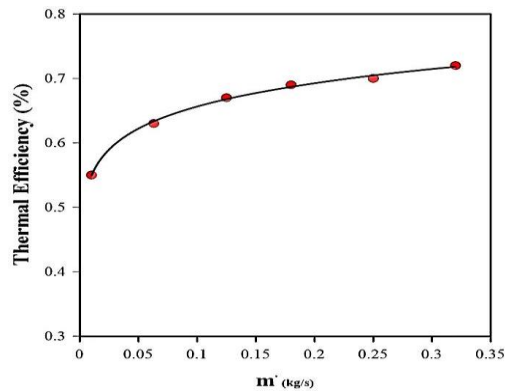**Figure 13.** Thermal efficiency versus mass flow rates at T_{in}=350K

Figure 14. Thermal efficiency versus mass flow rates at T_{in}=450K

4.6 Theoretical data for heat energy

Figure 15 displays the heat energy when the mass flow rate is (32 L and 45 L). The results indicated that when the mass flow rate was continuous, the amount of heat energy increased.
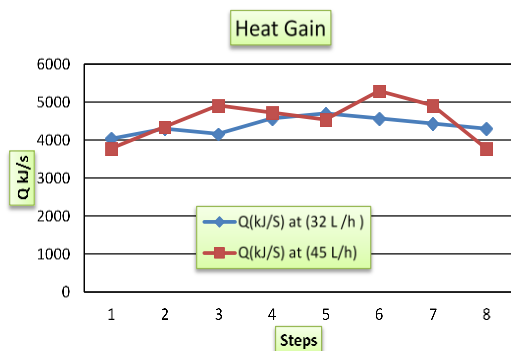

Figure 15. Heat energy gain for mass flow rates (32 L/hour, 45 L/hour)

5. CONCLUSIONS

Thermal performance investigation of PDC solar assisted cogeneration plant is presented in this study. The collected heat is further used to drive the steam cycle producing power and process heat simultaneously. The model is designed and simulated in the Ansys Workbench software for a different mass flow rate of the water in the receiver. The solar calculator is used to simulate the parabolic trough collector for solar loading. The major outcomes are presented as follows:

(1) The use of a radiator heat exchanger gives the largest use of solar reflected radiation that is reflected from the collector because of the increased surface area exposed to solar radiation due to the presence of fins.

(2) The PDC with water as an HTF has the highest thermal efficiency (72.16%) at 450 K and a mass flow rate of 0.32 kg/sec.

(3) It is found that the temperature of steam during the months of (June, and July) is more than during the months of (May, and April) as well as the results during the P.M., are better than A.M.

REFERENCES

[1] Frier, D., Cable, R.G. (1999). An overview and operation optimisation of the kramer junction solar electric generating system. In ISES World Congress, Jerusalem, 1: 241-246. http://dx.doi.org/10.1016/B978-008043895-5/50039-4

[2] Mills, D. (2004). Advances in solar thermal electricity technology. Solar Energy, 76(1-3): 19-31. https://doi.org/10.1016/S0038-092X(03)00102-6

[3] Sa'ad Al-deen, A.E. (2016). The performance assessment of a concentrating solar systems in Iraq. Al-Mustansiriyah University, requirements for the degree of Doctorate of Philosophy in Mechanical Engineering.

[4] Kalogirou, S.A. (2004). Solar thermal collectors and applications. Progress in Energy and Combustion Science, 30(3): 231-295. http://dx.doi.org/10.1016/j.pecs.2004.02.001

[5] Wu, S.Y., Xiao, L., Cao, Y., Li, Y.R. (2010). A parabolic dish/AMTEC solar thermal power system and its performance evaluation. Applied Energy, 87(2): 452-462. http://dx.doi.org/10.1016/j.apenergy.2009.08.041

[6] Dascomb, J. (2009). Low-cost concentrating solar collector for steam generation.

[7] Madadi, V., Tavakoli, T., Rahimi, A. (2014). First and second thermodynamic law analyses applied to a solar dish collector. Journal of Non-Equilibrium Thermodynamics, 39(4): 183-197. http://dx.doi.org/10.1515/jnet-2014-0023

[8] Li, L., Dubowsky, S. (2011). A new design approach for solar concentrating parabolic dish based on optimized flexible petals. Mechanism and Machine Theory, 46(10): 1536-1548. https://doi.org/10.1016/j.mechmachtheory.2011.04.012

[9] Lovegrove, K., Burgess, G., Pye, J. (2011). A new 500 m² paraboloidal dish solar concentrator. Solar Energy, 85(4): 620-626. https://doi.org/10.1016/j.solener.2010.01.009

[10] Mohammed, I.L. (2012). Design and development of a parabolic dish solar water heater. International Journal of Engineering Research and Applications, 2(1): 822-830.

[11] Rafeeu, Y., Ab Kadir, M.Z.A. (2012). Thermal performance of parabolic concentrators under Malaysian environment: A case study. Renewable and Sustainable Energy Reviews, 16(6): 3826-3835. https://doi.org/10.1016/j.rser.2012.03.041

[12] Karimi, S.O., Sadeghi, A.M.B., Khalilaria, S., Mirzaee, I. (2014). Two new designs of parabolic solar collectors. Thermal Science, 18(suppl. 2): 323-334. http://dx.doi.org/10.2298/TSCI111105089S

[13] Sakhare, V., Kapatkar, V.N. (2014). Experimental analysis of parabolic solar dish with copper helical coil receiver. Physics, Engineering, 1: 199-204.

[14] Sada, G.K.A., Sa'ad-Aldeen, A.E. (2015). Experimental steady to produce steam by solar energy using solar dish concentration with copper coil receiver. International Journal of Engineering and Innovative Technology (IJEIT), 4(7): 147-149.

[15] Mahmood, Y.H., Jassim, A.S., Hamed, F.N. (2017). Design and fabrication of Solar dish array and study it characterization. Tikrit Journal of Pure Science, 22(11): 2415-1726. http://dx.doi.org/10.25130/tjps.v22i11.920

[16] Khan, M.S., Abid, M., Ali, H.M., Amber, K.P., Bashir, M.A., Javed, S. (2019). Comparative performance assessment of solar dish assisted s-CO_2 Brayton cycle using nanofluids. Applied Thermal Engineering, 148: 295-306. http://dx.doi.org/10.1016/j.applthermaleng.2018.11.021

[17] Khan, M.S., Abid, M., Amber, K.P., Ali, H.M., Yan, M., Javed, S. (2021). Numerical performance investigation of parabolic dish solar-assisted cogeneration plant using different heat transfer fluids. International Journal of Photoenergy, 2021: 1-15. http://dx.doi.org/10.1155/2021/5512679

[18] Mari, M.A., Memon, Z.A., Shaikh, P.H., Mirjat, N.H., Uqaili, M.A. (2022). Numerical investigation to assess the output performance of concentrated solar parabolic dish system. Journal of Renewable and Sustainable Energy, 14(6): 063701. http://dx.doi.org/10.1063/5.0112533

[19] Spencer, G.H., Murty, M.V.R.K. (1962). General ray-tracing procedure. JOSA, 52(6): 672-678. http://dx.doi.org/10.1364/JOSA.52.000672

[20] Versteeg, H.K., Malalasekera, W. (1996). Introduction to computational fluid: The finite volume method. England: Longman Scientific & Technical.

[21] ANSYS FLUENT. (2013). Version 14.5, Ansys Inc.

[22] FLUENT Incorporated. (1998). Fluent 5 user's guide. Fluent Incorporated Lebanon, NH-USA.

[23] Benra, F.K., Dohmen, H.J., Pei, J., Schuster, S., Wan, B. (2011). A comparison of one-way and two-way coupling methods for numerical analysis of fluid-structure interactions. Journal of Applied Mathematics, 2011: 853560. https://doi.org/10.1155/2011/853560

[24] Al-damook, A., Azzawi, I.D. (2021). The thermohydraulic characteristics and optimization study of radial porous heat sinks using multi-objective computational method. Journal of Heat Transfer, 143(8). http://dx.doi.org/10.1115/1.4051126

[25] Ali, S.K., Azzawi, I.D., Khadom, A.A. (2021). Experimental validation and numerical investigation for optimization and evaluation of heat transfer enhancement in double coil heat exchanger. Thermal Science and Engineering Progress, 22: 100862. http://dx.doi.org/10.1016/j.tsep.2021.100862

[26] Faraj, A.F., Azzawi, I.D., Yahya, S.G. (2020). Pitch variations study on helically coiled pipe in turbulent flow region using CFD. International Journal of Heat and Technology, 38(4): 775-784. http://dx.doi.org/10.18280/ijht.380402

[27] Faraj, A.F., Azzawi, I.D., Yahya, S.G., Al-Damook, A. (2020). Computational fluid dynamics investigation of pitch variations on helically coiled pipe in laminar flow region. Journal of Heat Transfer, 142(10): 104503. http://dx.doi.org/10.1115/1.4047646

[28] Azzawi, I.D., Al-damook, A. (2022). Multi-objective optimum design of porous triangular chamber using RSM. International Communications in Heat and Mass Transfer, 130: 105774. http://dx.doi.org/10.1016/j.icheatmasstransfer.2021.105774

[29] Mohammed, K., Saleem, A., Obaid, Z.A.H. (2021). Numerical investigation of Nusselt number for nanofluids flow in an inclined cylinder. Frontiers in Heat and Mass Transfer (FHMT), 16. http://dx.doi.org/10.5098/hmt.16.20

[30] Omar, I., Alrudhan, A., Hammoodi, K.A., Mohammed Ali, A. (2020). Experimental and theoretical comparison between metallic and mirror reflectors with different receiver tank. Journal of Mechanical Engineering Research and Developments, 43(7): 51-61.